

Effect of surface roughness of the neutralization grid on the energy and flux of fast neutrals and residual ions extracted from a neutral beam source

Alok Ranjan

Plasma Processing Laboratory, Department of Chemical and Biomolecular Engineering,
University of Houston, Houston, Texas 77204-4004

Clemens Helmbrecht

University of Applied Sciences, Munich, Bavaria, D-80335 Germany

Vincent M. Donnelly^{a)} and Demetre J. Economou^{b)}

Plasma Processing Laboratory, Department of Chemical and Biomolecular Engineering,
University of Houston, Houston, Texas 77204-4004

Gerhard F. Franz

University of Applied Sciences, Munich, Bavaria, D-80335 Germany

(Received 18 October 2006; accepted 21 December 2006; published 29 January 2007)

A directional fast neutral beam was extracted from an inductively coupled argon plasma in contact with a neutralization grid. Ions expelled from the plasma converted into fast neutrals by grazing angle collisions with the internal surfaces of the openings of the grid. The effect of surface roughness of the neutralization grid was studied experimentally by using two grids: an array of holes drilled in an aluminum plate, and a set of atomically smooth Si parallel plates. With the atomically smooth Si grid, the ion translational energy lost in the surface collision was relatively small, and agreed well with the prediction of a specular reflection model. For the relatively rough metal grid, however, the translational energy loss was substantial due to the reduced probability of specular reflection from the rough surface. The residual ion flux and fast neutral flux were observed to be two to four times higher for the Si grid than for the metal grid, due to a higher percent open area and specular reflections off the smooth Si surfaces. The neutralization efficiency with the Si grid was between ~50% and 90%, depending on plasma conditions. At the highest neutral beam energies, the Si grid neutralizes about half of the incoming ions and thus would provide a sufficient flux of directional neutrals for anisotropic etching at commercially viable rates. © 2007 American Vacuum Society. [DOI: 10.1116/1.2433983]

I. INTRODUCTION

As microelectronic device dimensions continue to shrink, problems associated with conventional plasma etching (such as notching, aspect ratio dependent etching, and electrical damage to insulator films) are a serious concern.^{1–5} One way to reduce or eliminate these problems is to substitute directional fast (~100 eV) neutrals for the positive ions that cause anisotropic etching. This so-called neutral beam etching (NBE) has been the subject of continuing research.^{6–12} To make NBE practical on an industrial scale, the energy and flux of the fast neutrals need to be comparable to those of ions in reactive ion etching. To obtain a high flux of fast neutrals, Panda *et al.*¹³ and Samukawa *et al.*^{14–16} have used high density inductively coupled plasmas (ICP). Ions were expelled from the plasma through a grid with high aspect ratio holes. Ions turned into fast neutrals by undergoing glancing angle collisions with the internal surfaces of the grid holes. The resulting fast neutrals retained much of the parent ion energy and directionality.

The energy distributions of residual ions and fast neutrals, and the neutralization efficiency, were reported for different grid hole sizes and aspect ratios, as a function of pressure, power, and boundary voltage.¹⁷ The cylindrical high aspect ratio grid holes were formed by mechanical drilling, and were therefore rough on a microscopic scale. The energy lost upon conversion of ions to neutrals at glancing macroscopic angles was larger than that predicted for an atomically smooth surface.¹⁸ This discrepancy was attributed to the rough surface of the grid holes, which effectively made the true ion angle of incidence far from glancing.

To investigate the effect of surface roughness, the energy distribution and flux of fast neutrals and residual ions were measured with a grid composed of parallel, polished silicon plates that provided an atomically smooth surface for glancing angle neutralization. Results were compared with those obtained with a metal (aluminum) grid with holes having a relatively rough surface, used in a previous study.¹⁷

II. EXPERIMENT

The neutral beam source used in this study was similar to that of Panda *et al.*¹³ and was described earlier.¹⁷ The source consisted of an argon ICP with an ion “beam acceleration

^{a)}Electronic mail: vmdonnelly@uh.edu

^{b)}Electronic mail: economou@uh.edu

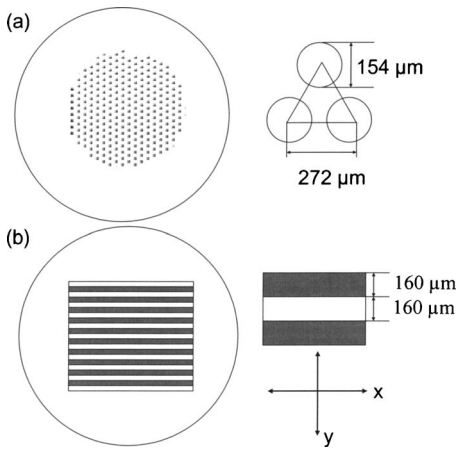


FIG. 1. Schematic of (a) metal (aluminum) grid with drilled holes, and (b) Si grid with parallel plates.

electrode,” in contact with the plasma. A fraction of the 13.56 MHz rf power of the ICP source was applied to the beam acceleration electrode to generate a “boundary voltage” (V_b). V_b was varied to control the ion energy and hence the fast neutral beam energy. The accelerated ions converted into fast neutrals by grazing angle collision with the internal surfaces of the holes of a grounded metal grid (neutralization grid). Pressure was set by adjusting the argon feed gas flow rate.

To study the effect of surface roughness of the neutralization grid on the energy distribution and flux of fast neutrals, two neutralization grids were used: one with relatively rough holes and one with atomically smooth (hereafter to be referred as “smooth”) plates. The grid with rough holes [Fig. 1(a)], used in the previous study,¹⁷ was an aluminum (6061, T6) disc, with cylindrical high aspect ratio holes drilled in a triangular pattern. The holes were 154 μm in diameter, with an aspect ratio of 7:1. Therefore, the maximum angle of ions exiting this grid without colliding with the walls was $\pm 8.1^\circ$ with respect to the hole axes. The distance between hole centers was 272 μm , yielding a transparency of 29%.

The smooth grid was fabricated from 1.08 \times 13 mm² rectangular strips of a thinned silicon wafer [160 μm thick, p type (100), polished on both sides]. The Si strips were slid into slots in a stainless steel plate to form a grid [Fig. 1(b)]. Silver paste was used to join the Si strips to the plate for better electrical contact. The plate spacing was 160 μm and the grid “thickness” was 1.08 mm. This resulted in an aspect ratio of 6.75:1 and a transparency of 50%. The Si grid transmitted ions with angles of up to $\pm 8.4^\circ$ with respect to the beam axis, perpendicular to the plane of the Si plates (y direction in Fig. 1), and all angles in the direction along the plates (x direction). Atomic force microscopy (AFM) images of the Si grid surface indicated a root mean square roughness of $\sim 1.5 \text{ Å}$. Scanning electron microscopy (SEM) images of the surface of the metal grid holes indicated roughness of $\sim 1 \mu\text{m}$.

The energy distribution of the fast neutral beam was measured by the same method as described previously.¹⁷ Briefly,

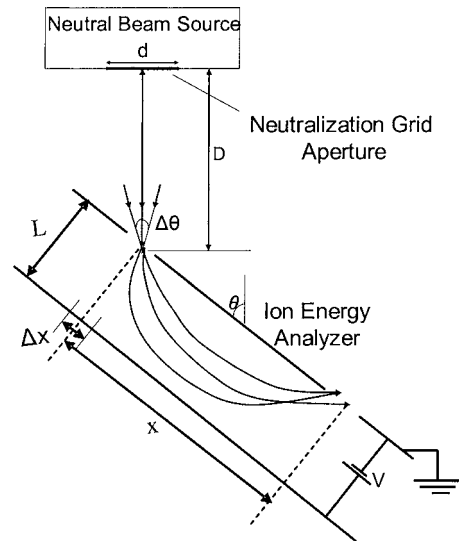


FIG. 2. Schematic of electrostatic ion energy analyzer underneath the neutralization grid (not to scale).

after removing residual Ar⁺ with a positively biased repeller grid, the directed Ar neutral beam was crossed with a pulsed electron beam. The ions created by electron impact ionization of fast neutrals were energy dispersed by a parallel-plate electrostatic analyzer (Fig. 2), and were detected with a channel electron multiplier. The weak modulated signal from ionized neutrals was distinguished from the strong, continuous background signal of mostly ultraviolet light, by phase sensitive detection with a lock-in amplifier. The same system was used to measure the energy distribution of residual ions that passed through the grid without colliding with the walls. In this mode, the repeller grid was grounded and the electron gun was switched off.

The open area of the neutralization grid was defined by a $d=5 \text{ mm}$ diameter aperture at a distance $D=35 \text{ mm}$ from the entrance slit of the electrostatic energy analyzer. Thus, the analyzer received ions (both primary plasma ions and fast neutrals ionized by the electron beam) at the center of the entrance slit at a maximum angle of $\pm 4^\circ$ [$\tan^{-1}(2.5 \text{ mm}/35 \text{ mm})$] with respect to the beam axis. Ions passed through the analyzer entrance slit and traveled in parabolic trajectories, covering different horizontal distances depending upon the incoming ion kinetic energy E (where it is understood that the ion energy is in eV), applied voltage between the plates V , and angle between the ion beam and the analyzer plates θ , given by¹⁹

$$E = \frac{Vx}{2L \sin 2\theta}, \quad (1)$$

where the angle θ is

$$\theta = \frac{1}{2} \sin^{-1} \left(\frac{Vx}{2LE} \right) \quad \text{or} \quad \theta = \frac{\pi}{2} - \frac{1}{2} \sin^{-1} \left(\frac{Vx}{2LE} \right). \quad (2)$$

Here $L=22.8 \text{ mm}$ was the separation between the plates, and $x=50 \text{ mm}$ was the distance between the slits. The width of the entrance and exit slits was $\Delta x=2 \text{ mm}$. For an ion energy

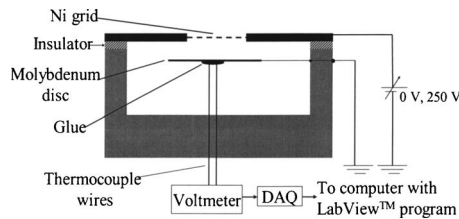


FIG. 3. Schematic of calorimeter.

and corresponding voltage between the plates, and for $\theta = 45^\circ$ and $x=50$ mm, ions entering the entrance slit at an angle between 39.3° and 50.7° (ions of $\Delta\theta = \pm 5.7^\circ$ divergence; see Fig. 2) could pass through the exit slit of the energy analyzer, covering 49 mm (corner of the exit slit) to 50 mm (center of the exit slit) of horizontal distance. Therefore, residual ions and ionized fast neutrals were detected up to a maximum angle of only $\pm 4^\circ$ for both grids in both the x and y directions, limited by the 5 mm diameter aperture on the neutralizer grid.

Absolute energy fluxes (W/cm^2) were measured with a homebuilt calorimeter (Fig. 3), similar to one used by Kersten *et al.*²⁰ The calorimeter was a 12 mm diameter molybdenum disc with a thickness, h , of 0.1 mm. A low sputter rate and high corrosion resistance made molybdenum a good choice for the disc. When energetic particles strike the Mo disc, they deposit most of their energy in the disc as heat. The calculations carried out by Helmer and Graves¹⁸ for Ar⁺ impacting Si can be used to estimate the percent energy transfer from normal incidence Ar ions and fast neutrals to the Mo calorimeter. The authors found that 50 eV ions at normal incidence reflected 41% of the time. These ions deposited 83% of their energy to the surface. The remaining 59% of ions penetrated the surface and therefore deposited 100% of their energy. Therefore, one would expect $\sim 92\%$ of the incident energy of impinging species to be transferred to the Mo disc. Given the relatively rough surface of the Mo disc, the energy transfer should exceed 92%. For simplicity, a 100% energy transfer from the impinging species to the disk was assumed.

When a flux of energetic particles was initiated, the temperature of the Mo disc increased with time. The temperature rise was measured with a fine gauge thermocouple (50 μm diameter wire) that was bonded to the back of the Mo disc with thermally conducting and electrically insulating cement (Fig. 3). Electrical current from the beam had no influence on the temperature measurement. The disc was suspended with three fine wires (not shown) to minimize heat losses by conduction. These wires also connected the disc to ground, eliminating any possibility for charging of the disc. A 90% open area Ni grid was placed above the disk. This grid was either positively biased to reject positive ions and allow only neutrals to strike the Mo disc, or grounded to allow the total flux of residual ions and neutrals to strike the disc.

The procedure for measuring energy fluxes with the calorimeter was as follows: After the plasma was ignited and the desired conditions established, a shutter that blocked the

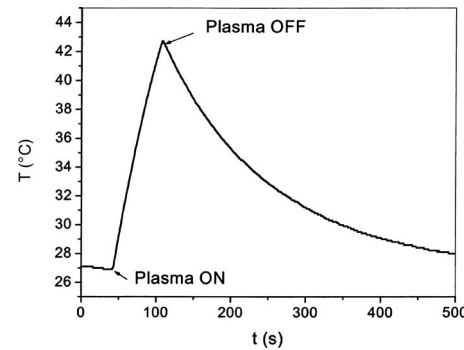


FIG. 4. Temperature response of thermocouple attached to the calorimeter for Si grid with plasma on (conditions: 150 W power, 10 mTorr pressure, and 50 V boundary voltage) and plasma off.

beam was opened. The temperature of the metal disc T increased, due to bombardment by high energy neutrals (and ions if allowed to pass through the Ni grid). After some time the rf power was turned off and T decreased due to heat losses. A typical temperature versus time t curve for the Si grid (10 mTorr Ar plasma, 150 W power, $V_b=50$ V) is shown in Fig. 4. The heat flux Γ_H is given by

$$\Gamma_H = \frac{hA\rho C_p}{A_p} \left[\left(\frac{dT}{dt} \right)_{\text{heat}} - \left(\frac{dT}{dt} \right)_{\text{cool}} \right]_{T=T_S}, \quad (3)$$

where $(dT/dt)_{\text{heat}}$ and $(dT/dt)_{\text{cool}}$ are the time derivatives of the disc temperature during heating (exposed to beam) and cooling (beam off), measured at the same temperature, T_S (see Fig. 4), C_p is the heat capacity of Mo (0.25 J/g K), ρ is the density of Mo (10.28 g/cm³) at room temperature, and $h=0.1$ mm. The cross sectional area of the Mo disc was $A = 1.131$ cm² and the area of the aperture at the front of the calorimeter was $A_p=0.78$ cm².

The measured heat fluxes were divided by the mean energy to determine the beam flux. The mean energy $\langle E \rangle$ was calculated by

$$\langle E \rangle = \frac{\int_0^\infty f(E)EdE}{\int_0^\infty f(E)dE}, \quad (4)$$

where $f(E)$ is the energy distribution function of the fast neutral beam or residual ion beam measured with the electrostatic analyzer.

III. RESULTS AND DISCUSSION

Energy distributions measured with the electrostatic analyzer are presented in Fig. 5 for a 150 W, 10 mTorr plasma with a boundary voltage $V_b=50$ V. The residual ion energy distributions (IED) for the two grids (solid squares) are nearly the same, as expected. In contrast, the neutral energy distributions (NED) for the two grids are quite different. The peak in the NED, relative to the IED, is 3 eV lower for the Si plate grid, and 14 eV lower for the metal hole grid. In addition, the population of low energy neutrals (below 50 eV) is

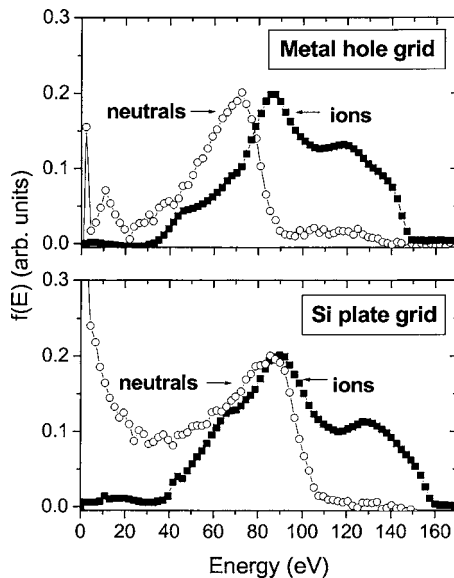


FIG. 5. Residual ion energy distributions and fast neutral energy distributions for the Si grid and metal grid. Conditions: 150 W power, 10 mTorr pressure, and 50 V boundary voltage.

considerably higher with the Si grid. Neither grid generates high energy neutrals (>110 eV), despite the fact that there is a substantial population of ions at these higher energies.

These observations can be explained as follows. Ions near the peak of the IED undergoing glancing angle collisions with the smooth Si grid are much more likely to scatter specularly and lose little energy compared to those scattered from the rough metal grid surfaces. For the same reason, neutrals are more likely to make several bounces off the smooth, parallel Si grid surfaces and emerge as lower energy (<50 eV) neutrals with relatively low angular spread. Finally, the highest energy ions (>110 eV) have the narrowest angular distribution. They preferentially pass through the grid without colliding with the walls, hence few neutrals are produced by these ions.

When an atom specularly scatters from a surface at an incident angle, θ_i (with respect to the surface normal), its kinetic energy, ε_r , after reflection is related to its incident kinetic energy, ε_i , by the expression¹⁸

$$\sqrt{\frac{\varepsilon_r}{\varepsilon_i}} = \left(\frac{\mu}{\mu + 1} \right)^2 \left(\cos \chi_{1/2} + \sqrt{\frac{1}{\mu^2} - \sin^2 \chi_{1/2}} \right)^2, \quad (5)$$

where $\mu = m_{\text{Ar}}/m_{\text{wall}}$ is the ratio of the atomic mass of Ar to that of the wall material (ignoring the oxide coating and assumed to be the atomic masses of Al and Si for the two grids), and $\chi_{1/2} = \pi/2 - \theta_i$. [Equation (5) corresponds to two successive binary collisions of the impinging ion with surface atoms.] Using this expression for ions with $\varepsilon_i = 89$ eV (peak energy) and $\theta_i = 84^\circ$ (corresponding to a 6° divergence with respect to the vertical, as obtained from particle-in-cell simulations²¹), a shift of only 2.8 eV was predicted for the scattered neutrals. This is in excellent agreement with the 3 eV observed for the smooth Si plate grid. The much larger shift observed for the rough metal hole grid can be attributed

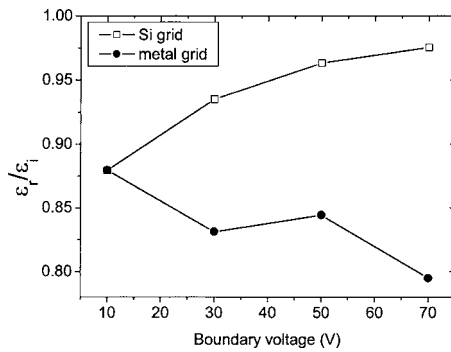


FIG. 6. Fraction of incident ion energy retained by scattered neutrals as a function of boundary voltage for the Si grid and metal grid. Conditions: 150 W power and 10 mTorr pressure.

to the roughness of the surface of the grid holes.

Figure 6 presents ratios of the measured peak neutral energy to the peak residual ion energy as a function of V_b . At low energy ($V_b = 10$ V) both grids behave similarly. As energy increases, however, the $\varepsilon_r/\varepsilon_i$ ratios bifurcate—increasing with V_b for the Si grid while decreasing for the metal grid. As V_b is increased, the incoming ions become more directional hence, from Eq. (5), $\varepsilon_r/\varepsilon_i$ is expected to increase, as observed for the smooth Si grid. For the rough metal grid, Eq. (5) is not expected to be applicable, as observed in the contrary behavior of $\varepsilon_r/\varepsilon_i$ with increasing V_b . It was also found that $\varepsilon_r/\varepsilon_i$ for the Si grid was nearly independent of power (0.99 at 150 W to 1.01 at 350 W, with 10 mTorr and $V_b = 50$ V). This can be explained by a comparison of the grid hole openings, D , with the sheath thickness, L_{sh} . When $D \gg L_{\text{sh}}$, the plasma “molds” into the grid openings and ions are strongly deflected toward the grid walls. On the other hand, when $D < L_{\text{sh}}$ the plasma does not significantly penetrate into the grid openings. Simulations²² and prior experiments¹⁷ have shown that for these plasma conditions and a 154 μm cylindrical hole grid, the latter condition holds. Plasma molding would be even less important for the one-dimensional (1D) (i.e., parallel plate) grid used in the present study. Finally, $\varepsilon_r/\varepsilon_i$ for the Si grid increased weakly with increasing pressure (0.98 at 10 mTorr to 1.05 at 40 mTorr, with 150 W and $V_b = 50$ V). Pressure is expected

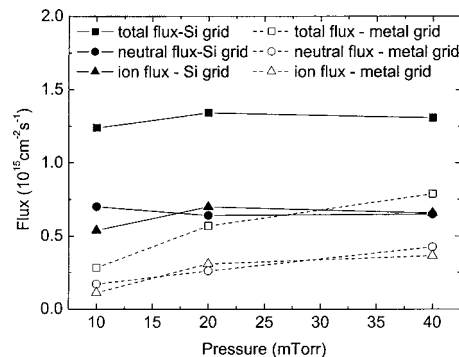


FIG. 7. Total flux, residual ion flux, and fast neutral flux for Si grid and metal grid, as a function of pressure. Conditions: 150 W power and 50 V boundary voltage.

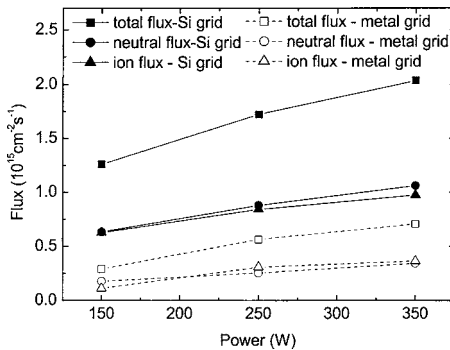


FIG. 8. Total flux, residual ion flux, and fast neutral flux for Si grid and metal grid, as a function of power. Conditions: 10 mTorr pressure and 50 V boundary voltage.

to affect ϵ_r/ϵ_i in many ways, through its effect on plasma electron temperature and density, sheath thickness, molding over the grid, and charge exchange in the presheath and downstream of the grid.

Figures 7–9 present total, fast neutral, and residual ion fluxes for both grids as a function of plasma gas pressure, power, and boundary voltage. Several overall trends can be gleaned from these data. All fluxes increase with increasing power, because of the higher ion number density at the plasma-grid boundary. Most importantly, the Si plate grid transmitted two to four times the flux of fast neutrals compared to the metal hole grid, with the largest advantage offered at low pressure and high power. This is substantially above the 1.7-fold higher transparency (50%/29%) of the Si grid. The added neutral flux with the Si grid was most likely due to the more specular reflections on the smooth Si surface. The added ion flux can be ascribed to the reduced probability for collisions in the 1D Si plate grid as opposed to the two dimensional (2D) metal hole grid. The flux of residual ions through the Si grid increases strongly with V_b while all other fluxes are relatively unaffected (Fig. 9). This is again consistent with the smaller ion angular spread at higher V_b . Also, as V_b increases, the sheath thickness increases and plasma molding becomes weaker, making ion flow through the grid holes more directional. Figures 7–9 show that the degree of neutralization with the Si grid (ratio of fast neutral

flux to the sum of the fast neutral and residual ion fluxes) is between about 50% and 90%. It should be pointed out that even at the highest values for V_b , which would provide sufficiently high energy for anisotropic etching, the Si grid neutralizes about half of the incoming ions and thus would provide a sufficient flux of directional neutrals.

IV. SUMMARY

The energy distribution and flux of fast neutrals and residual ions extracted from a neutral beam source were measured using two different neutralization grids: one with relatively rough holes drilled through an aluminum disk, and one with atomically smooth parallel surfaces made from pieces of thinned, double-side polished Si wafers. For the same plasma conditions, ion energy distributions for both grids were nearly the same. Ions undergoing glancing angle collisions with the smooth Si grid walls were scattered specularly. The energy loss of ions scattered on the Si grid to become fast neutrals was in good agreement with the predictions of a specular reflection model. The corresponding energy loss was much greater for the metal grid; specular reflection is a poor approximation for the scattering from this rough surface.

The residual ion flux and fast neutral flux were observed to be two to four times higher for the Si grid than for the metal grid. The higher transparency of the Si grid explains, in part, the higher fluxes. The smoothness of the Si surface and resulting specular reflection could explain the additional fast neutral flux. The reduced probability for collisions in the (1D) Si plate grid as opposed to the (2D) metal hole grid is consistent with the additional ion flux. The neutralization efficiency with the Si grid was between about 50% and 90%.

ACKNOWLEDGMENTS

This work was supported by the Texas Advanced Technology Program. Many thanks to Manish K. Jain for AFM and SEM images. C.H. and G.F. thank the German National Science Foundation for financial support.

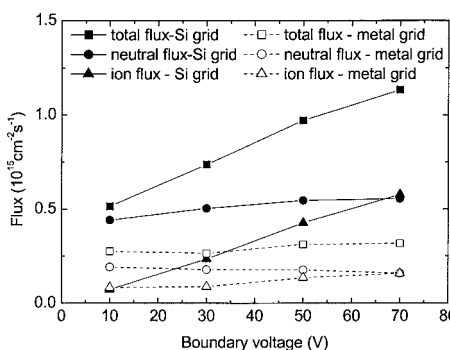


FIG. 9. Total flux, residual ion flux, and fast neutral flux for Si grid and metal grid, as a function of boundary voltage. Conditions: 150 W power and 10 mTorr pressure.

- ¹S. Samukawa, Appl. Phys. Lett. **64**, 3398 (1994).
- ²N. Fujiwara, T. Maruyama, and M. Yoneda, Jpn. J. Appl. Phys., Part 1 **35**, 2450 (1996).
- ³G. S. Hwang and K. P. Giapis, J. Appl. Phys. **82**, 566 (1997).
- ⁴D. J. Economou and R. Alkire, J. Electrochem. Soc. **135**, 941 (1988).
- ⁵J. C. Arnold and H. H. Sawin, J. Appl. Phys. **70**, 5314 (1992).
- ⁶H. Kuwano and F. Shimokawa, J. Vac. Sci. Technol. B **6**, 1565 (1988).
- ⁷F. Shimokawa, H. Tanaka, Y. Uenishi, and R. Sawada, J. Appl. Phys. **66**, 2613 (1989).
- ⁸T. Mizutani and T. Yunogami, Jpn. J. Appl. Phys., Part 1 **29**, 2220 (1990).
- ⁹T. Yunogami, K. Yogokawa, and T. Mizutani, J. Vac. Sci. Technol. A **13**, 952 (1995).
- ¹⁰K. Yokogawa, T. Yunigami, and T. Mizutani, Jpn. J. Appl. Phys., Part 1 **35**, 1901 (1996).
- ¹¹T. Tsuchizawa, Y. Jin, and S. Matsuo, Jpn. J. Appl. Phys., Part 1 **33**, 2200 (1994).
- ¹²Y. Jin, T. Tsuchizawa, and S. Matsuo, Jpn. J. Appl. Phys., Part 2 **34**, 465 (1995).
- ¹³S. Panda, D. J. Economou, and L. Chen, J. Vac. Sci. Technol. A **19**, 398 (2001).
- ¹⁴S. Samukawa, K. Sakamoto, and K. Ichiki, J. Vac. Sci. Technol. A **20**, 1566 (2002).

- ¹⁵S. Noda, H. Nishimori, T. Iida, T. Arikado, K. Ichiki, T. Ozaki, and S. Samukawa, *J. Vac. Sci. Technol. A* **22**, 1506 (2004).
- ¹⁶H. Otake, N. Inoue, T. Ozaki, and S. Samukawa, *J. Vac. Sci. Technol. B* **23**, 210 (2005).
- ¹⁷A. Ranjan, V. M. Donnelly, and D. J. Economou, *J. Vac. Sci. Technol. A* **24**, 1839 (2006).
- ¹⁸B. A. Helmer and D. B. Graves, *J. Vac. Sci. Technol. A* **16**, 3502 (1998).
- ¹⁹G. D. Yarnold and H. C. Bolton, *J. Sci. Instrum.* **26**, 38 (1949).
- ²⁰H. Kersten, D. Rohde, J. Berndt, H. Deutsch, and R. Hippler, *Thin Solid Films* **377–378**, 585 (2000).
- ²¹S. K. Nam, D. J. Economou, and V. M. Donnelly, *J. Phys. D* **39**, 3994 (2006).
- ²²D. Kim and D. J. Economou, *IEEE Trans. Plasma Sci.* **30**, 2048 (2002).